

PAPER • OPEN ACCESS

## Which is better, electrostatic or piezoelectric energy harvesting systems?

To cite this article: A D T Elliott *et al* 2015 *J. Phys.: Conf. Ser.* **660** 012128

View the [article online](#) for updates and enhancements.

### You may also like

- [Charging power optimization for nonlinear vibration energy harvesting systems subjected to arbitrary, persistent base excitations](#)  
Quanqi Dai and Ryan L Harne
- [Force and stability mechanism analysis of two types of nonlinear mono-stable and multi-stable piezoelectric energy harvesters using cantilever structure and magnetic interaction](#)  
Shuailing Sun, Yonggang Leng, Sunghoon Hur et al.
- [Maximum power point of piezoelectric energy harvesters: a review of optimality condition for electrical tuning](#)  
A Brenes, A Morel, J Juillard et al.

# Which is better, electrostatic or piezoelectric energy harvesting systems?

A D T Elliott<sup>1</sup>, L M Miller<sup>2</sup>, E Halvorsen<sup>3</sup>, P K Wright<sup>4</sup> and P D Mitcheson<sup>1</sup>

<sup>1</sup> Department of Electrical and Electronic Engineering, Imperial College London, London, UK

<sup>2</sup> Alphabet Energy, Eden Landing Rd, Hayward, CA, USA

<sup>3</sup> Buskerud and Vestfold University College, Grønland 58, 3045 Drammen, Norway

<sup>4</sup> University of California, Berkeley, CA, USA

E-mail: alwyn.elliott07@imperial.ac.uk

**Abstract.** This paper answers the often asked, and until now inadequately answered, question of which MEMS compatible transducer type achieves the best power density in an energy harvesting system. This question is usually poorly answered because of the number of variables which must be taken into account and the multi-domain nature of the modelling and optimisation. The work here includes models of the mechanics, transducer and the power processing circuits (e.g. rectification and battery management) which in turn include detailed semiconductor models. It is shown that electrostatic harvesters perform better than piezoelectric harvesters at low accelerations, due to lower energy losses, and the reverse is generally true at high accelerations. At very high accelerations using MEMS-scale devices the dielectric breakdown limit in piezoelectric energy harvesters severely decreases their performance thus electrostatics are again preferred. Using the insights gained in this comparison, the optimal transduction mechanism can be chosen as a function of harvesting operating frequency, acceleration and device size.

## 1. Introduction

Vibrational energy harvesters are often considered as an alternative to batteries for wireless sensors as once installed the harvester does not require regular maintenance. However the choice of transducer (e.g. electrostatic or piezoelectric) to use to convert the mechanical vibration into electrical energy isn't always obvious due to variation in dominance of various loss mechanisms and material constraints. A comparison of the full system models for both electrostatic and piezoelectric energy harvesters is therefore required in order to select the correct transduction method in a given situation.

Electrostatic energy harvesters extract power by using mechanical vibrations to separate charged plates, causing work to be done against the electrostatic attraction. Many examples of MEMS scale electrostatic energy harvesters have been modelled and fabricated [1, 2]. They can be divided into two main types, constant charge, and constant voltage. These harvesters have then been modelled for optimisation in [3, 4], however [3] assumes an optimal resistive load is connected to the output therefore ignoring the constraints due to the low power conditioning circuit required, and [4] ignores analysis of the circuit efficiency. Instead the constant voltage model presented in [5] is preferred and used here as it generates a fully parametrised model. Note



the constant charge implementation is ignored as its performance was shown to be worse than constant voltage in [5].

Piezoelectric energy harvesters extract power by inducing a voltage across the piezoelectric material when mechanical stress from a vibration is applied. Examples of piezoelectric energy harvesters can be found in [6], however fully modelling a piezoelectric energy harvester system is more difficult as the type of power conditioning circuit and the limitations these impose have to be taken into account. In [7], the single-supply pre-biasing (SSPB) circuit was shown to outperform all other power conditioning circuits, however the models used did not take into account the effect of the damping force on the transducer. The full system model presented in [8] was therefore chosen for comparison as the same model parametrisation as in [5] is used.

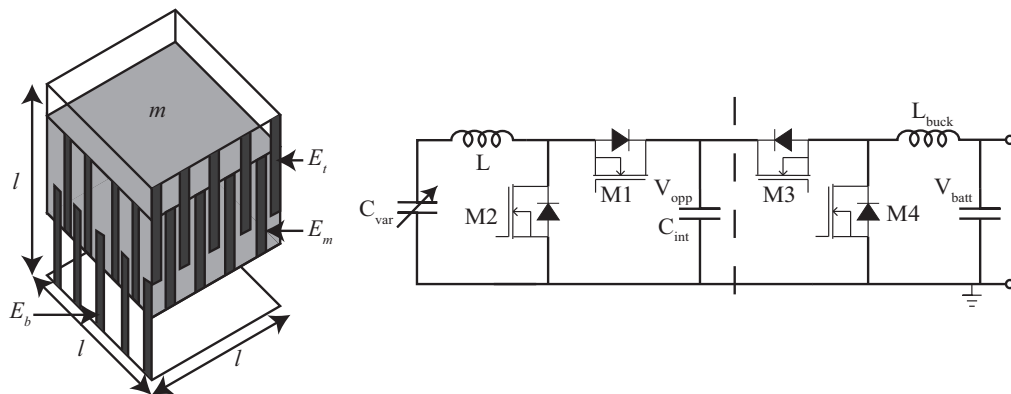
This paper reveals when to use an electrostatic or piezoelectric energy harvesting system for a given harvesting operating frequency, acceleration and device size. The paper first presents the models and algorithms for each transduction method. The maximum power generation and system effectiveness at 100 Hz operating frequency for both transducers are then compared enabling an engineer to choose an optimal transduction mechanism for a given application.

## 2. Background

Electrostatic and piezoelectric energy harvesters have been modelled using the mass-spring-damper model and electrical equivalent circuits for each has been derived previously [9, 7]. Both the electrostatic and piezoelectric energy harvesters have been shown to preferably be operated as Coulomb damped resonant generators (CDRGs) [10, 11]. The advantage of this is the electrical damping force may be set by applying a fixed voltage making it very easy to control and set to the optimal value.

### 2.1. Electrostatic model

Figure 1 (a) shows the physical structure of the constant voltage electrostatic energy harvester. The top and bottom electrodes ( $E_t$  and  $E_b$ ) alternatively mesh together with the mass electrode,  $E_m$ , as the applied mechanical excitation oscillates the mass vertically. For more details see [5].



(a) Constant voltage physical configuration (b) Constant voltage power conditioning circuit

**Figure 1.** Mechanical configuration and power conditioning circuit for constant voltage electrostatic energy harvester based on [5].

The power conditioning circuit required to implement the constant voltage configuration is shown in Figure 1 (b). Switches M3 and M4 act as a boost circuit to prime the intermediate capacitor,  $C_{int}$ , to the optimal voltage ( $V_{opp}$ ). The voltage on  $C_{var}$  is then increased by pulsing

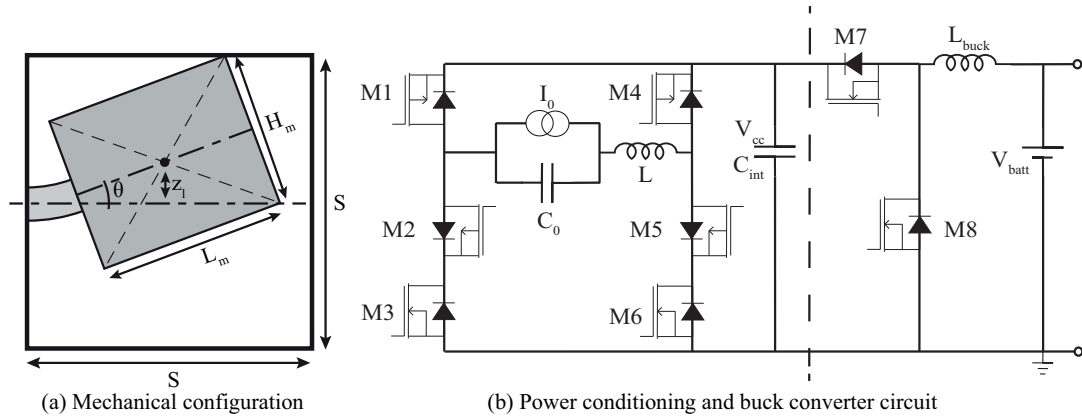


**Figure 2.** Mechanical structure and power conditioning circuit for piezoelectric energy harvesting system [8].

switch M1 until the voltage on  $C_{\text{var}}$  is equal to  $V_{\text{opp}}$ . The electrodes move apart, causing almost all the charge to be transferred from  $C_{\text{var}}$  to  $C_{\text{int}}$  through M1. As the electrodes move back together again M1 is opened and M3 and M4 are operated as a buck circuit to transfer the extracted energy to the storage element,  $V_{\text{supply}}$  [5].

### 2.2. Piezoelectric model

The mechanical structure of the piezoelectric transducer is assumed to be a simple cantilever beam with a proof mass on the end (Figure 2 (a)). The beam consists of a piezoelectric thin film with silicon and oxide structural layers. The displacement of the mass is calculated to ensure that the deflection of the beam does not cause the mass to collide with side of the box.

The most compact circuit capable of operating a piezoelectric energy harvester as a CDRG is the single-supply pre-biasing (SSPB) circuit (Figure 2 (b)) [12]. This circuit transfers charge from an intermediate storage capacitor,  $C_{\text{int}}$ , to the piezoelectric layer on the cantilever when it reaches its extreme points of travel in order to pre-bias it through a set of switches (e.g. M1, M5, M6). This pre-bias charge induces a Coulomb-damping force which acts in the opposite direction to the motion of the cantilever, therefore increasing the work done. As the cantilever deflects to the opposite extreme point, more charge is induced. The pre-bias and induced charge are then returned back to  $C_{\text{int}}$  through the same set of switches used to pre-bias (e.g. M1, M5, M6) before the pre-bias is applied with the opposite polarity through the other set of switches (e.g. M4, M2, M3). Switches M7 and M8 are used to transfer extracted energy from  $C_{\text{int}}$  to the storage battery,  $V_{\text{batt}}$ , to maintain the optimal voltage on  $C_{\text{int}}$ .

### 2.3. System effectiveness

A harvester's maximum theoretically available power at a given acceleration ( $A_{\text{input}}$ ), with a volume of side length  $S$ , at an operating frequency ( $\omega_{\text{input}}$ ) and proof mass density ( $\rho_{\text{mass}}$ ) [10] is

$$P_{\text{max}} = \frac{1}{16} \rho_{\text{mass}} A_{\text{input}} \omega_{\text{input}} S^4. \quad (1)$$

The effectiveness of a harvesting system can thus be calculated by dividing the final output power,  $P_{\text{out}}$ , of the harvesting system by the maximum available power:

$$\eta_{\text{system}} = \frac{P_{\text{out}}}{P_{\text{max}}}. \quad (2)$$

### 3. Model Implementations

Several assumptions were made about both systems to help constrain the problem for comparison. Firstly the displacement of the mass was not allowed to exceed the given volume as this would cause damage to device. The inductor is assumed to occupy half the given volume of the device. The proof mass was assumed to be made of gold as it is compatible with MEMS manufacturing techniques and has a high density ( $19320 \text{ kg m}^{-3}$ ). The 1.5 V battery, used to store the extracted energy, is assumed the same size and hence excluded as part of the system volume. All semiconductor devices are assumed to be small enough as to occupy negligible space.

#### 3.1. Electrostatic algorithm

The electrostatic model algorithm operates as follows. First the operating frequency,  $\omega_{\text{input}}$ , and vectors for side length,  $S$ , and acceleration,  $A_{\text{input}}$ , are defined. The optimal operating voltage for given  $S$  and  $A_{\text{input}}$  is then found. If this voltage exceeds semiconductor device breakdown the pre-charge voltage is reduced. Numerical solutions for  $\eta_{\text{system}}$  using different numbers of semiconductor cells are then calculated. The optimal number of cells which maximises  $\eta_{\text{system}}$  is thus selected. The algorithm is repeated with the next value of  $S$  and  $A_{\text{input}}$ . For more detail on the algorithm see [5].

#### 3.2. Piezoelectric algorithm

The piezoelectric model algorithm is similar to the electrostatic model and operates as follows. First the operating frequency,  $\omega_{\text{input}}$ , and vectors for side length,  $S$ , and acceleration,  $A_{\text{input}}$ , are defined. Beam length and thickness pairs are then found which resonate within 1 % of  $\omega_{\text{input}}$ . Using these beam definitions, the transducer parameters are calculated. The optimal pre-bias voltage required for CDRG operation and the end voltage after beam deflection are then calculated. If the end voltage exceeds piezoelectric dielectric breakdown, the displacement of the mass is decreased. Initial numerical solutions for the circuit's parameters are then calculated for different circuit inversion efficiencies. The circuit parameters are then iteratively updated to allow for charge sharing, leakage and conduction losses in the SSPB and buck circuits. The net power and system effectiveness are finally calculated. The algorithm is repeated with the next value of  $S$  and  $A_{\text{input}}$ . For more detail on the algorithm see [8].

### 4. Results

The comparison of the two systems was performed at 100 Hz with the volume constrained between 1 mm and 15 mm and the acceleration varied between  $0.01 \text{ ms}^{-2}$  to  $100 \text{ ms}^{-2}$  using a gold proof mass. The semiconductor device breakdown voltage was assumed to be 1.5 kV and the piezoelectric dielectric breakdown voltage was assumed to be 750 V.

Figure 3 compares the power output and system effectiveness for both energy harvesting systems. It can be clearly seen that the electrostatic system is preferred at low accelerations over the piezoelectric system as the energy losses in the piezoelectric devices at low power levels severely reduces the output power. As mechanical acceleration is increased, the electrostatic system requires increasingly high biasing voltages, causing the semiconductor device on-state resistance to increase in order to block the higher voltage, resulting in increased conduction losses and a preference for the piezoelectric system. However at very high accelerations the power output of the piezoelectric system is severely limited as the dielectric breakdown voltage in MEMS scale devices forces the mass displacement to be decreased thus not utilising the maximum deflection possible, therefore the electrostatic devices are preferred in this case.

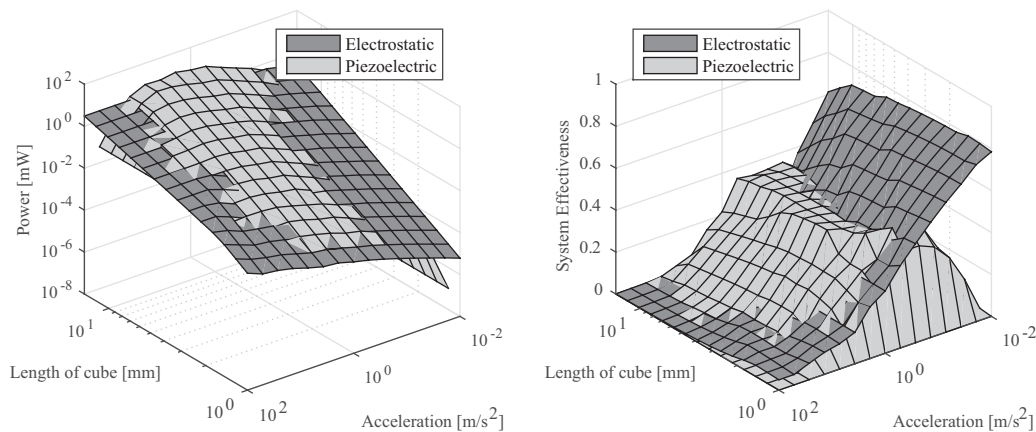


**Figure 3.** Comparison of the power output and system effectiveness between electrostatic and piezoelectric MEMS scale energy harvesting systems.

## 5. Conclusion

A full system model comparison of electrostatic and piezoelectric energy harvesters has been presented for the first time. It is clear that at very low accelerations, electrostatic devices are preferred as they have lower losses. As the damping force and therefore required optimal biasing voltage increases, piezoelectric devices have better performance due to increased conduction losses than electrostatic devices, however at very high accelerations MEMS scale piezoelectric material suffer from voltage breakdown thus electrostatic devices should be used. Future work therefore should examine larger devices where bulk piezoelectric material can be used as it has a higher breakdown voltage. A comparison with electromagnetic resonant vibrational energy harvesting systems should also be conducted in order to compare all three technologies.

## Acknowledgements

The authors would like to thank the California Energy Commission and Research Council of Norway grant number 229716 and for their support, and EPSRC for their sponsorship of this project through a doctoral training award at Department of Electrical and Electronic Engineering, Imperial College London.

## References

- [1] Suzuki Y 2011 *IEEJ Transactions on Electrical and Electronic Engineering* **6** 101–111 ISSN 1931-4981
- [2] Le C P and Halvorsen E 2012 *Journal of Micromechanics and Microengineering* **22** 074013
- [3] Mitcheson P D, Reilly E K, Toh T, Wright P K and Yeatman E M 2007 *J. Micromech. Microeng* **17** S211
- [4] Guillemet R, Basset P, Galayko D and Bourouina T 2010 *Procedia Engineering* **5** 1172 – 1175 ISSN 1877-7058 eurosensor {XXIV}
- [5] Mitcheson P and Green T 2012 *Circuits and Systems I, IEEE Transactions on* **59** 3098–3111 ISSN 1549-8328
- [6] Kim H, Kim J H and Kim J 2011 *INT J PRECIS ENG MAN* **12** 1129–1141 ISSN 1229-8557
- [7] Dicken J, Mitcheson P D, Stoianov I and Yeatman E 2012 *Power Electronics, IEEE Transactions on* **27** 4514–4529 ISSN 0885-8993
- [8] Miller L M, Elliott A D T, Mitcheson P D, Halvorsen E, Paprotny I and Wright P K UNDER REVIEW *IEEE Transactions on Circuits and Systems - Part 1*
- [9] Mitcheson P D and Toh T T 2010 Power management electronics *Energy Harvesting for Autonomous Systems* (Norwood, MA: Artech House, Inc) chap Chapter 6
- [10] Mitcheson P, Green T, Yeatman E and Holmes A 2004 *Microelectromechanical Systems, Journal of* **13** 429–440 ISSN 1057-7157
- [11] Miller L M, Mitcheson P D, Halvorsen E and Wright P K 2012 *Applied Physics Letters* **100** 233901
- [12] Dicken J, Mitcheson P D, Elliott A D T and Yeatman E M 2011 Single-supply pre-biasing circuit for low-amplitude energy harvesting application *PowerMEMS* (Seoul, South Korea) pp 46–49